Proceedings of the 17th World Congress
The International Federation of Automatic Control
Seoul, Korea, July 6-11, 2008

Mass Measurement under Weightless Conditions by Relay Feedback Systems

Takeshi MIZUNO*, Masaya TAKASAKI, Yuji ISHINO*****

**Department of Mechanical Engineering, Saitama University, Shimo-Okubo 255, Sakura-ku, Saitama 338-8570, Japan (Tel: +81-48-858-3455; e-mail: mizar@mech.saitama-u.ac.jp)*
***Department of Mechanical Engineering, Saitama University, Shimo-Okubo 255, Sakura-ku, Saitama 338-8570, Japan (Tel: +81-48-858-3451; e-mail: masaya@mech.saitama-u.ac.jp)*
****Department of Mechanical Engineering, Saitama University, Shimo-Okubo 255, Sakura-ku, Saitama 338-8570, Japan (Tel: +81-48-858-3453; e-mail: yishinor@mech.saitama-u.ac.jp)*

Abstract: The applicability of relay feedback to mass measurement was investigated. Two mass measurement systems were studied both theoretically and experimentally. One of them uses an on-off relay with hysteresis and switches force acting on the object in relation to the velocity of the object. The other contains an on-off relay with dead zone and switches force acting on the object in relation to the displacement. The principle of measurement, a fabricated apparatus and measurement results were presented for each measurement system.

1. INTRODUCTION

Various weightless experiments have been conducted to find new phenomena that could not be observed on earth. The production of new materials and medicines in space is expected to start in the near future. Mass measurement under such special conditions will be necessary to perform next-stage space experiments and start pioneering productions.

Several measurement systems have been already proposed (Mizuno 2003). However, no decisive method has been established yet. Not only measurement accuracy but also weight reduction should be considered for actual operation in space.

Mizuno *et al.* (2002) has proposed to apply relay feedback to mass measurement under weightless conditions for achieving measurement with a simple mechanism. Two types of measurement systems are possible (Mizuno 2002 and Mizuno *et al.* 2005). One of them contains an on-off relay with hysteresis and switches force acting on the object in relation to the velocity of the object (velocity-feedback type); the mass of the object is determined from the period of the oscillation. The other contains an on-off relay with dead zone and switches force acting on the object in relation to the displacement (displacement-feedback type); the mass of the object is determined from the time interval measurement of the on-state and off-state periods. The principle measurement, a fabricated experimental apparatus and several measurement results of each system are presented.

2. VELOCITY-FEEDBACK TYPE

2.1 Principles

Figure 1a shows a physical model for studying the principles of mass measurement, and Fig.1b shows the block diagram of the control system of velocity-feedback type (Mizuno *et al.*, 2002). It is made up of four elements:

(1) actuator for moving a measurement object,
(2) sensor for detecting the velocity of the object,
(3) controller for producing switching signals,
(4) amplifier for driving the actuator.

The operation of the measurement system is shown in Fig.2. The force $F(t)$ produced by the actuator is switched in relation to the velocity v of the object by a relay element with hysteresis. When the force applied to the mass is F_0, the velocity of the object increases. When the velocity reaches a preset threshold value v_0, the applied force is changed from F_0 to $-F_0$. Then the velocity decreases. When the velocity reaches the other threshold value $-v_0$, the applied force is changed from $-F_0$ to F_0. When the actuator is controlled in this way, a periodic oscillation is excited as shown in Fig.2.

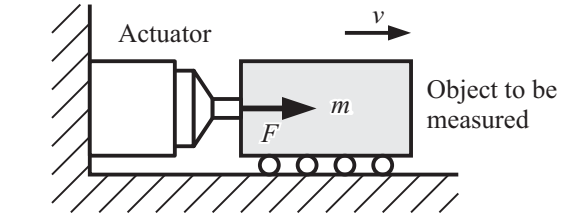

(a) Physical model

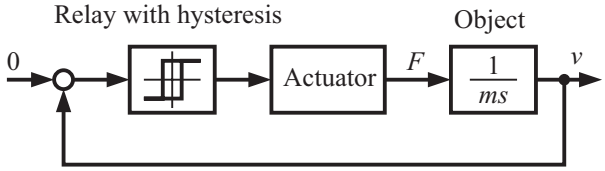

(b) Control system

Fig.1 Velocity-feedback type measurement system

The period of the oscillation is designated as T. When the applied force is F_0, the equation of motion is given by

$$m\ddot{x} = F_0 . \tag{1}$$

Solving (1) with $\dot{x}(0) = -v_0$ leads to

$$2v_0 = \frac{F_0}{m} \cdot \frac{T}{2}, \tag{2}$$

From (2), we get

$$m = \frac{F_0}{4v_0} T . \tag{3}$$

Therefore, the mass of the measurement object can be estimated by measuring T.

2.2 Experimental System

Figure 3 shows a schematic drawing of an apparatus developed for experimental study (Mizuno *et al.*, 2007). It uses a voice coil motor (VCM) as an actuator for moving the object. Another VCM is installed for generating disturbance. The movers are connected with a mechanical coupling. An object to be measured is attached to the movers.

The maximum displacement and output force of the VCM's are 15[mm] and 9.8[N], respectively. They are driven by current-control power amplifiers.

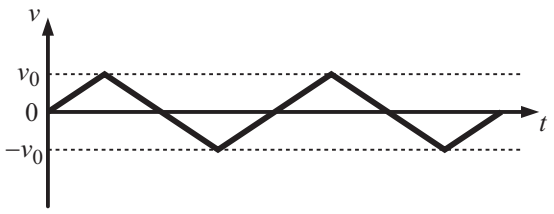

(a) Velocity of the object

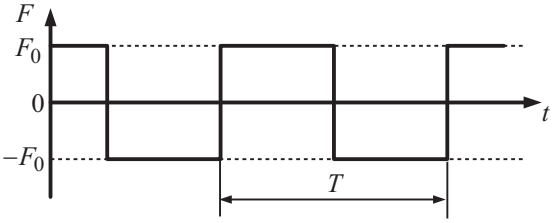

(b) Force acting on the object

Fig.2 Operation of the measurement system

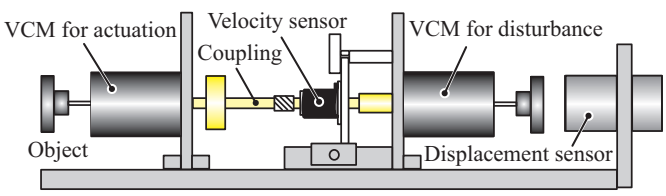

Fig.3 Schematic drawing of experimental apparatus

In actual measurement, a spring-like element must be added for avoiding the drift of the mover. In this work, the VCM for disturbance is controlled to operate as a spring by feeding back the displacement of the mover. Its stiffness is designated by k_c.

A velocity sensor was fabricated in which a permanent magnet moves inside windings to induce back electromotive force in the coil. The permanent magnet is attached to the coupling. The voltage across the coil e is proportional to the velocity of the permanent magnet.

The control algorithm described in the previous section is implemented with a DSP-based digital controller. The velocity signal is inputted to the controller through an A/D converter. The controller generates binary command signal ($\pm I_0$) so as to operate as an on-off relay with hysteresis whose width is given by $\pm v_0$ (see Fig.2). This signal is sent to the power amplifier through a D/A converter. The electromagnetic force is switched to be $\pm F_0$ alternatively so that the measurement object oscillates as shown in Fig.2. The period T of this oscillation is measured with a digital oscilloscope.

2.3 Experimental Results

First, the effects of the parameter F_0 on the measurement accuracy are experimentally studied. Figure 4 shows measurement results for nine samples from 297.0[g] to 409.0[g] when $v_0 = 40$[mm/s] and $k_c = 0.78$[kN/m] and F_0 is set as

(a) $F_0 = 1.88$[N], (b) $F_0 = 1.97$[N],
(c) $F_0 = 2.11$[N], (d) $F_0 = 2.20$[N],
(e) $F_0 = 2.30$[N].

In this figure, the period of the limit cycle is plotted for each measurement mass. The obtained data were fitted to a straight line by the least-squares method and the deviation from this line was estimated in each case. The deviation from the line was smallest in the case of (d). In the following, therefore, F_0 is set to be 2.20[N].

Next, the effects of the parameter v_0 on measurement accuracy are studied. Figure 5 shows the results when $k_c = 1.56$[kN/m] and v_0 is set as

(a) $v_0 = 30$[mm/s], (b) $v_0 = 40$[mm/s],
(c) $v_0 = 50$[mm/s], (d) $v_0 = 60$[mm/s].

The deviation from a fitted line was smallest in the case of (d) where the line is obtained as

$$m = 11.5 \times T\,[\mathrm{ms}] - 49.6\,[\mathrm{g}] . \tag{4}$$

In the following, therefore, v_0 was set to be 60[mm/s].

Another measurement was again carried out to check the effectiveness of the calibration based on (4). Nine samples from 297.0[g] to 409.0[g] are measured again. Figure 6 compares the original estimation based on (3) with the estimation calibrated according to (4). It indicates that appropriate calibration is necessary for accurate measurement. The relative error e of the calibrated estimation m_c is calculated according to

$$e = \frac{m_c - m_r}{m_r} \times 100 \quad [\%]. \tag{5}$$

The maximum and the average of their absolute values are 0.7[%] and 0.4[%], respectively.

Figure 6 indicates that mass is estimated to be smaller than actual without the calibration. Mizuno *et al.* (2008) show that the main factor of this discrepancy is the stiffness k_c.

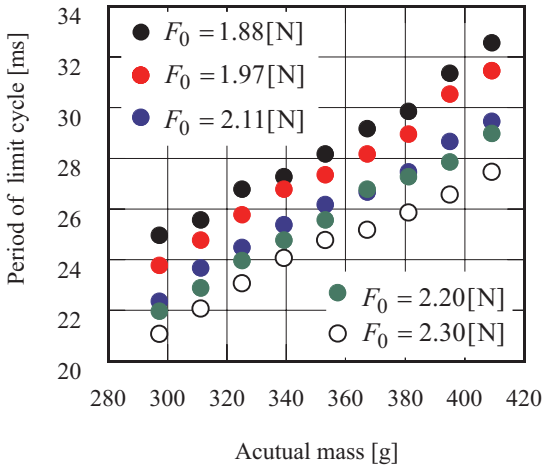

Fig.4 Relation between mass and period when F_0 is varied.

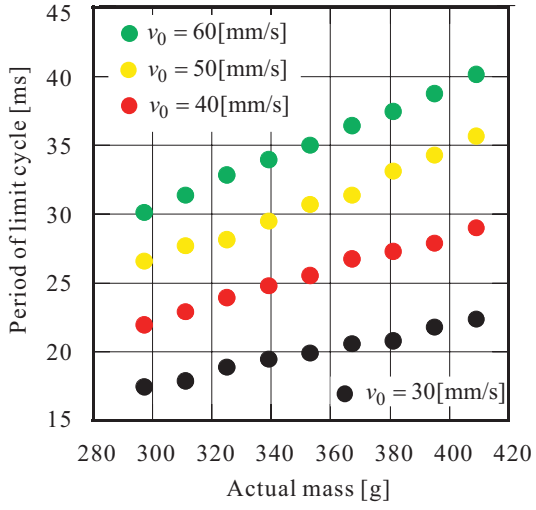

Fig.5 Relation between mass and period when v_0 is varied.

3. DISPLACEMENT-FEEDBACK TYPE

3.1 Principles

In the displacement-feedback type, the sensing element is replaced by a displacement sensor. It is to be mentioned that compact and low-cost sensors such as photo interrupter are available. This is an advantage over the velocity-feedback type. Figure 7 shows a block diagram of its control system (Mizuno *et al.*, 2005). The operation of the measurement system is shown in Fig.8. The force $F(t)$ produced by the generator is switched in relation to the displacement x of the object to satisfy

$$F(t) = -F_0, \quad \text{when} \quad X_0 \le x, \tag{6}$$

$$F(t) = 0, \quad \text{when} \quad -X_0 < x < X_0, \tag{7}$$

$$F(t) = +F_0, \quad \text{when} \quad x \le -X_0. \tag{8}$$

Then a periodic oscillation is excited as shown in Fig.9. The periods during which $F = \pm F_0$ and $F = 0$ are designated as T_1 (on-state period) and T_2 (off-state period) respectively. The mass is assumed to pass the threshold positions $-X_0$ at velocities of $-V_0$. When $F(t) = F_0$, the equation of motion is given by

$$m\ddot{x} = F_0. \tag{9}$$

Solving (9) with $\dot{x}(0) = -V_0$ leads to

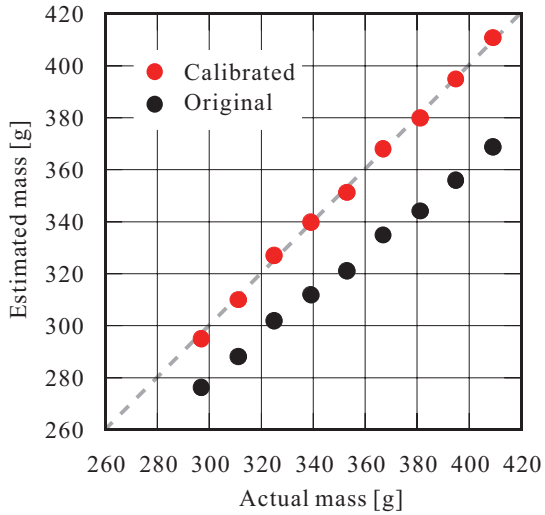

Fig.6 Comparison of the calibrated value with the original

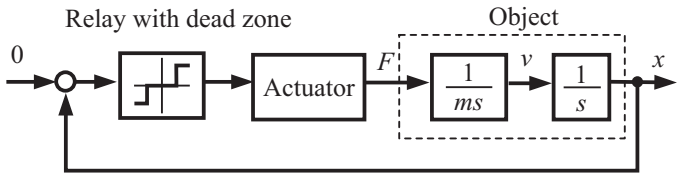

Fig.7 Block diagram of another measurement system.

$$2V_0 = \frac{F_0}{m} \cdot \frac{T_1}{2} . \quad (10)$$

When $F(t) = 0$, the equation of motion is given by

$$m\ddot{x} = 0 . \quad (11)$$

Solving (11) with $\dot{x}(t) = V_0 \ (0 \le t \le T_2 / 2)$ and $x(0) = -X_0$ leads to

$$2X_0 = V_0 \cdot \frac{T_2}{2} . \quad (12)$$

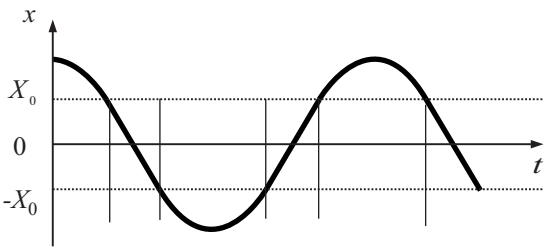

(a) Displacement of the mass

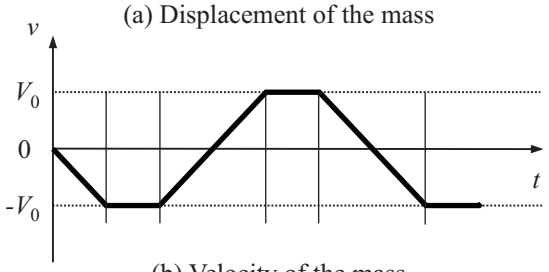

(b) Velocity of the mass

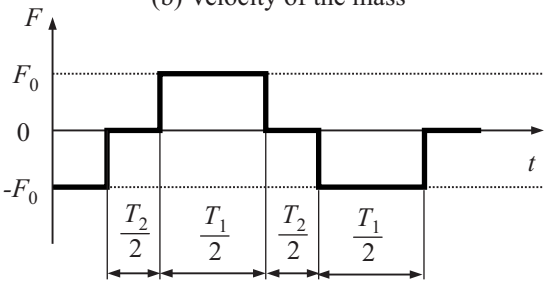

(c) Force acting on the mass

Fig.8 Operation of the measurement system

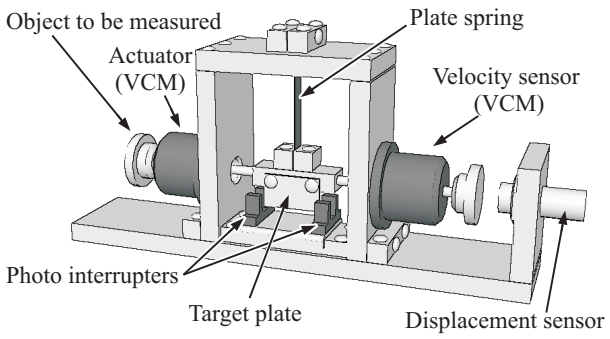

Fig.9 Experimental apparatus

Combining (10) with (12) leads to

$$m = \frac{F_0}{16X_0} T_1 T_2 . \quad (13)$$

Therefore, the mass of measurement object is determined from the time interval measurement of T_1 and T_2.

3.2 Experimental System

Figure 9 show a schematic drawing of an apparatus developed for experimental study on the position-feedback type (Mizuno *et al.*, 2005). A pair of photo detectors is used to detect the switching positions. The value of X_0 is adjusted by changing the width of the target plate that is attached to the object. The control algorithm given by (6) to (8) is implemented with a DSP-based digital controller.

Another VCM and an eddy-current gap sensor are installed for monitoring the displacement and velocity of the object. The VCM is also used to generate disturbances such as stiffness and damping to study their effects.

The movers of the VCM's are connected mechanically. Although no drift is expected in this system, the movers are guided by a plate spring to prevent them from rotating. Such rotation may disturb the detection of switching positions.

3.3 Operation of Measurement System

Figure 10 shows the applied force, velocity and displacement of the mover when $F_0 = 7.81[\mathrm{N}]$ and $X_0 = 1.5[\mathrm{mm}]$. It is observed that velocity decreases when $F(t) = 0$ ($|x| \le X_0$). This tendency is more apparent when F_0 is small (Mizuno *et al.*, 2005). The main factor of the decrease of velocity is friction in the VCM's. Figure 11 shows the closed trajectory of the control system when the force is switched as shown by Fig.12. The periodic motion was quite stable.

3.4 Measurement Results

The effects of the parameters X_0 and F_0 on measurement accuracy are experimentally studied. Figure 13 shows measurement results for 13 samples from 356.6[g] to 418.2[g] when X_0 is fixed to 1[mm] and F_0 is set as

(a) $F_0 = 1.95[\mathrm{N}]$, (b) $F_0 = 4.88[\mathrm{N}]$, (c) $F_0 = 7.81[\mathrm{N}]$.

In this figure, the measured value m_e versus the actual one m_r is plotted where the latter is determined with a high accuracy balance with a resolution of 1[mg]. The linearity is best in the case of (c).

Figure 14 shows measurement results when F_0 is fixed to 4.88N and X_0 is set as

(a) $X_0 = 0.5[\mathrm{mm}]$, (b) $X_0 = 1.0[\mathrm{mm}]$, (c) $X_0 = 1.5[\mathrm{mm}]$.

The ratio of T_1 to T_2 becomes

(a) $T_1 : T_2 \cong 4:1$, (b) $T_1 : T_2 \cong 1:1$, (c) $T_1 : T_2 \cong 1:3$.

The linearity is best in the case of (b).

These results indicate that F_0 should be large and the ratio of T_1 to T_2 should be one to one for accurate measurement. Thereby, another measurement was carried out when F_0 and X_0 were set as $F_0 = 9.37$[N] and $X_0 = 1.25$[mm] that made the ratio of T_1 to T_2 about one to one. The obtained data are fitted to a straight line by the least-squares method as

$$m_r = 5.58 + 1.016 m_e \text{ [g]} \tag{16}$$

Another measurement was again carried out to check the effectiveness of the calibration based on (16). Figure 15 compares the calibrated value m_r with the original estimation m_e. The maximum and the average of the errors of the calibrated estimation are 0.18[%] and 0.10[%], respectively.

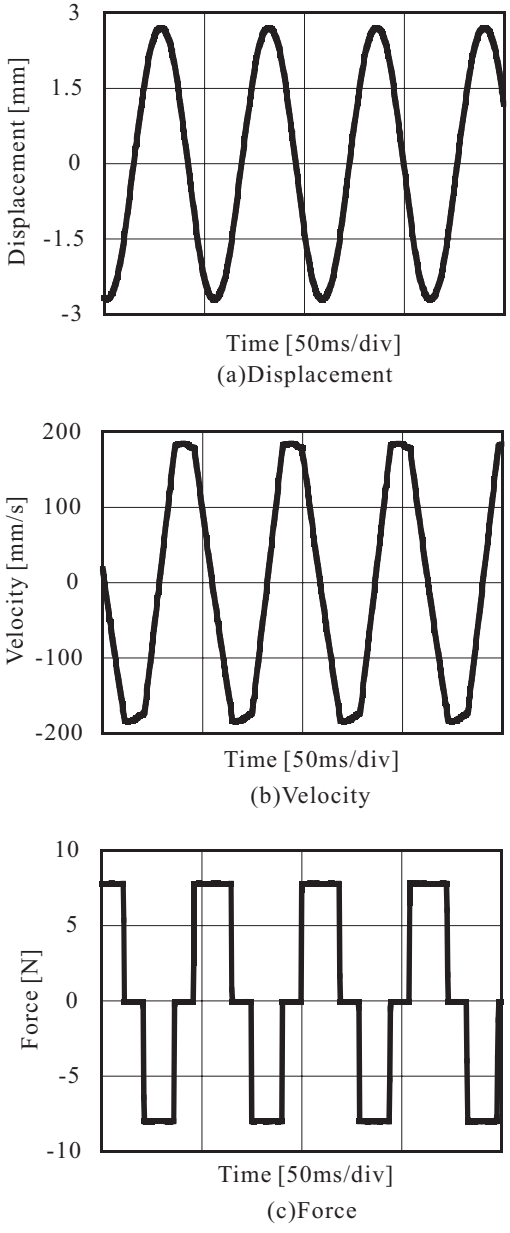

Fig.10 Operation of the control system

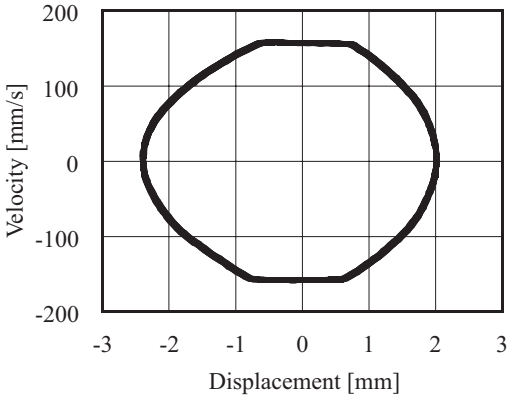

Fig.11 Closed trajectory of the control system

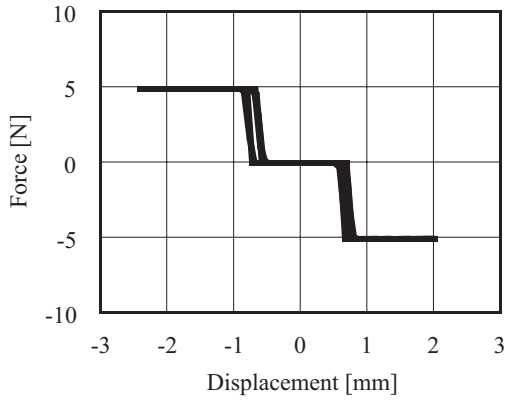

Fig.12 Force switched to the displacement

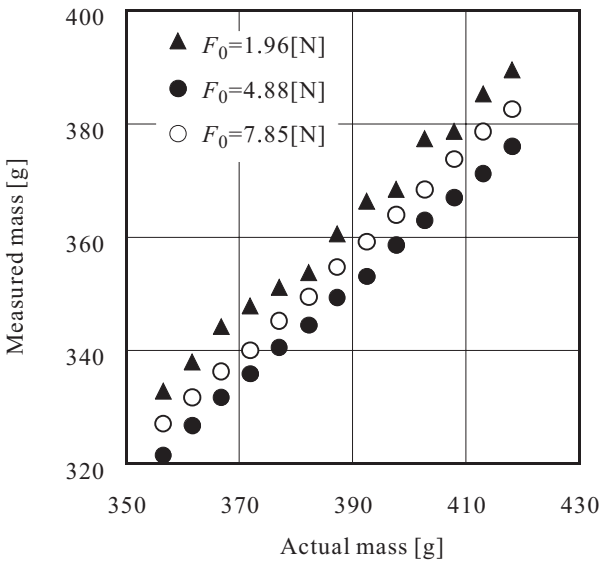

Fig.13 Measurement results when $X_0 = 1.0$[mm].

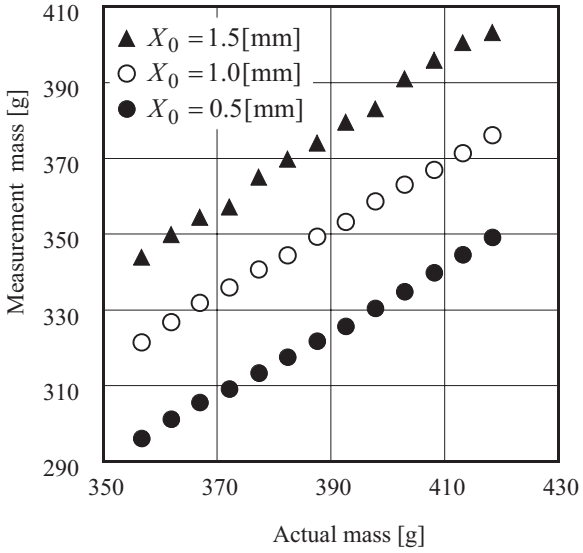

Fig.14 Measurement results when $F_0 = 4.88$[N].

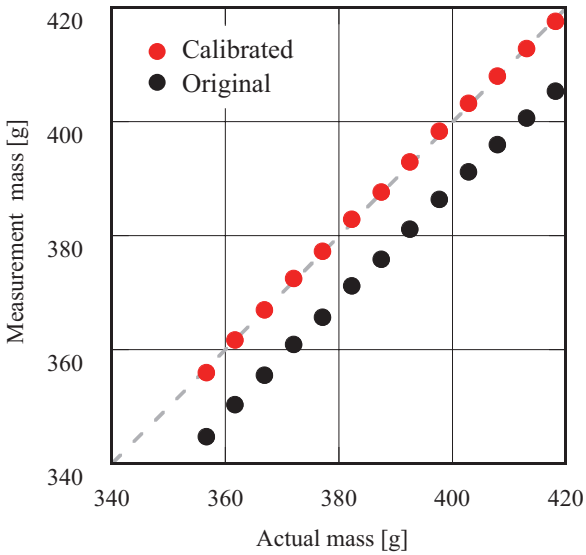

Fig.15 Comparison of the calibrated value with the original.

3.5 Effects of Stiffness

Figure 15 indicates that mass is estimated to be smaller than actual without calibration. One factor in this discrepancy is the effect of the plate spring for preventing the movers from rotating as mentioned in *Experimental System*. To estimate its effect, the VCM for velocity sensing is operated as a spring whose stiffness is designated by k_c. Figure 16 shows the measurement results. It is found that the estimated values become smaller as stiffness is higher.

CONCLUSIONS

Two mass measurement systems using relay feedback were compared. One of them contains an on-off relay with hysteresis and feeds back the velocity of the object. The other contains an on-off relay with dead zone and feeds back the position of the object. The principle of measurement of each type was clarified. Several mass measurements were carried out with the fabricated apparatuses. They showed that the latter had smaller measurement errors than the former.

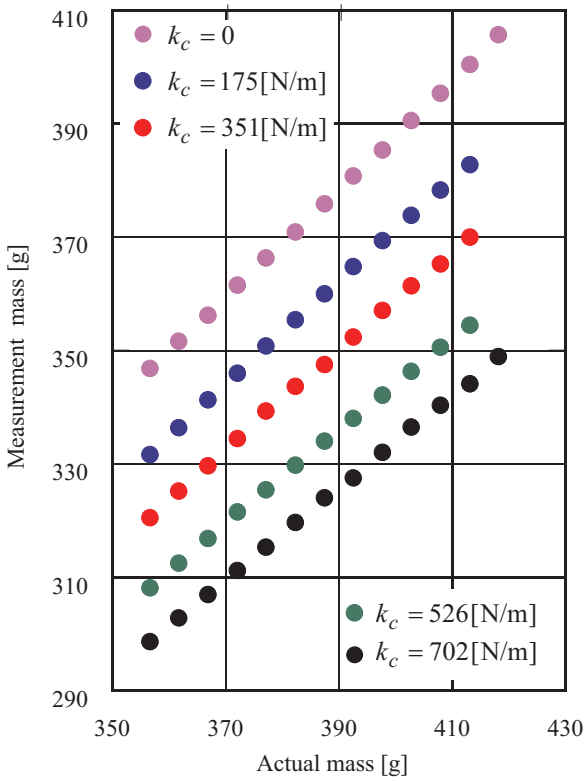

Fig.16 Effects of stiffness

REFERENCES

Mizuno, T., Yaoita, J., Takeuchi, M. and Takasaki, M. (2002). Mass Measurement Using the Self-Excited Vibration of a Relay Control System, *Proc. 6th Int. Conf. Motion and Vibration Control*, pp.807-811.

Mizuno, T. (2003). Devices for Mass Measurement under Weightless Conditions, *Proc. SICE Annual Conference 2003 in Fukui*, pp.245-251.

Mizuno, T., Takeuchi, M., Takasaki, M. and Ishino, Y. (2005). Mass Measurement Using a System Containing an On-Off Relay with Dead Zone, *Trans. the Society of Instrument and Control Engineering*, **41**, 1, pp.1-6.

Mizuno, T., Adachi, T., Takasaki, M. and Ishino, Y. (2007). Experimental Study on a Mass Measurement System Using a Relay with Hysteresis, *Proc. Asia-Pacific Vibration Conference 2007*, G04-2-5.

Mizuno, T., Ishino, Y. and Takasaki, M. (2008). Analysis on the Effect of Stiffness on Mass Measurement Using a Relay Feedback of Velocity, *Submitted to SICE Annual Conference 2008*.